Appl. Phys. B 65, 505–509 (1997)

Applied Physics B Lasers and Optics

Absorption gratings in ferroelectric $Bi_4Ti_3O_{12}$

X. Yue[1], **F. Mersch**[1], **R.A. Rupp**[2], **E. Krätzig**[1]

[1] Fachbereich Physik der Universität Osnabrück, Barbarastr. 7, D-49069 Osnabrück, Germany
[2] Institut für Experimentalphysik der Universität Wien, Boltzmanngasse 5, A-1090 Wien, Austria

Received: 10 February 1997

Abstract. Light-induced absorption changes are measured in ferroelectric $Bi_4Ti_3O_{12}$. Basic properties of absorption gratings in this crystal are investigated with beam-coupling experiments. Depending on the grating spacing, wavelength, and intensity of the writing beams, an absorption grating in our sample can be either in phase or shifted by 180° with respect to the light pattern. The formation mechanism of absorption grating is discussed and proposed to originate from a shallow-trap effect.

PACS: 42.70.L; 42.40.-i; 78.20.-e

Bismuth titanate ($Bi_4Ti_3O_{12}$) was studied with regard to its use in ferroelectric optical memory devices in the 1970s because its domain patterns are optically detectable and can be structured with high resolution [1, 2]. It has recently been found that holographic recording and beam coupling can be realized in this crystal [3, 4]. Three gratings were observed during holographic recording. There is a primary refractive-index grating with fast response and a phase shift of 90° with respect to the light pattern. It is compensated by a complementary refractive-index grating with much slower response. The third grating which can be identified by beam-coupling experiments is an absorption grating whose origin is not yet clear. The relative amplitude of the absorption grating and its phase relation compared with the refractive-index gratings are important for holographic applications as well as characterization of this photorefractive material. The basic properties of the absorption grating in $Bi_4Ti_3O_{12}$ and its formation mechanism are studied and discussed in this paper.

1 Experimental methods

1.1 Sample and experimental setup

The $Bi_4Ti_3O_{12}$ sample used in our present experiments is the same one as in our previous paper in which the extinction spectrum is given [3]. The entrance-face dimensions are 4.65 mm × 7.90 mm, and the thickness along the *c*-axis is 0.76 mm. The experimental arrangement is shown in Fig. 1. An argon-ion laser is used to write gratings for beam coupling experiments or functions as a pump for light-induced absorption measurements, whereas a weak He-Ne laser is used to monitor diffraction efficiency and light-induced absorption change. The transmitted and diffracted beam intensities are detected by photodiodes, amplified, and recorded with the help of a storage oscilloscope. The polarizations and intensities of the laser beams are controlled by two Soleil-Babinet compensators and polarizers. The sample is fixed to a crystal holder which can be shifted by a piezoelectric transducer along the course of the *a*-axis. The crystal holder is a copper plate to minimize potential heating by the intense pump-laser light during measurement of light-induced absorption changes.

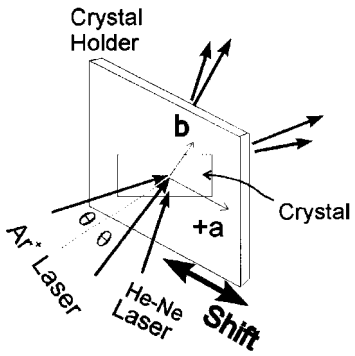

Fig. 1. Experimental configuration: two beams of an Ar^+ laser record a grating in a $Bi_4Ti_3O_{12}$ crystal and the beam of a He-Ne laser (in-Bragg) is diffracted from this grating

1.2 Light-induced absorption

In light-induced absorption measurements, the intensity of a transmitted weak He-Ne laser beam ($\lambda = 632.8$ nm) is recorded with and without the pump beam I_R ($\lambda = 514.5$ nm).

The light-induced absorption coefficient is defined as

$$\alpha_{\mathrm{li}} = \frac{1}{d} \ln \frac{I_{\mathrm{p}} \text{ without pump}}{I_{\mathrm{p}} \text{ with pump}} \tag{1}$$

where I_{p} is the intensity of the transmitted probe beam and d the effective crystal thickness. In order to block scattered light of the intense pump beam, a 632.8-nm interference filter is put in front of the photodetector. Under the above definition, $\alpha_{\mathrm{li}} > 0$ corresponds to light-induced absorption, whereas $\alpha_{\mathrm{li}} < 0$ indicates light-induced transparency.

The intensity of the pump beam is varied from 0.5 to 20 W/cm^2, while the intensity of the weak He-Ne probe beam is kept below 100 μW/cm^2.

1.3 Separation of an absorption grating from refractive-index gratings

Absorption gratings can be separated from refractive-index gratings by the beam-coupling method [5, 6]. After steady state has been reached during holographic recording, the sample is shifted at constant speed along the grating vector, so that the imposed external shift increases linearly with time and both writing beams become periodically modulated due to the varying direction of energy transfer. If translation time is much shorter than the time necessary to build up new gratings and diffraction efficiencies are low, the output-beam intensities as functions of the displacement ζ are [5]:

$$I_{\mathrm{R}}(\zeta) = I_{\mathrm{R0}}\, \mathrm{e}^{-\frac{\alpha d}{\cos(\theta_{\mathrm{i}})}} \left[1 - 2A\cos\left(\frac{2\pi\zeta}{\Lambda} + \Phi_{\mathrm{A}}\right) - 2P\sin\left(\frac{2\pi\zeta}{\Lambda} + \Phi_{\mathrm{P}}\right)\right], \tag{2}$$

$$I_{\mathrm{S}}(\zeta) = I_{\mathrm{S0}}\, \mathrm{e}^{-\frac{\alpha d}{\cos(\theta_{\mathrm{i}})}} \left[1 - 2A\cos\left(\frac{2\pi\zeta}{\Lambda} + \Phi_{\mathrm{A}}\right) + 2P\sin\left(\frac{2\pi\zeta}{\Lambda} + \Phi_{\mathrm{P}}\right)\right] \tag{3}$$

with the parameters

$$P = \frac{\pi \Delta n\, d}{\lambda \cos(\theta_{\mathrm{i}})}, \qquad A = \frac{\Delta\alpha\, d}{4\cos(\theta_{\mathrm{i}})}. \tag{4}$$

Here, $\Delta\alpha$ and Δn are the amplitudes of absorption and refractive index gratings, Φ_{A} and Φ_{p} are their phases with respect to the light pattern, α is the absorption coefficient, λ the vacuum wavelength of the writing beams, Λ the grating spacing, θ_{i} the half beam crossing angle inside the crystal, and I_{R0} and I_{S0} are the intensities of the incoming beams which are chosen to be equal in our experiments. Amplitudes and phases of absorption and refractive-index gratings can be obtained from the analysis of $I_{\mathrm{R}}(\zeta)$ and $I_{\mathrm{S}}(\zeta)$ using the above equations.

In our sample, as mentioned in the introductory paragraph, there are three gratings involved in holographic recording. However, amplitude and phase of the absorption grating can be determined correctly by the above technique, even though two refractive-index gratings contribute to beam coupling. In addition, the primary and complementary refractive-index gratings have very different response times [4], so that we can always choose a proper translation speed and a time interval which is much larger than the response time of the fast primary refractive-index grating, but nevertheless much smaller than the response time of the other two gratings. Under these conditions, the primary grating does not contribute to the variation of both coupling beams during translation of the sample after the primary grating has reached the steady state. This allows us to also determine amplitude and phase of the complementary refractive-index grating.

2 Experimental results

2.1 Light-induced absorption measurements

A typical variation of the transmission of a weak red probe beam with and without pump beam ($I_{\mathrm{R}} = 10$ W/cm^2) at room temperature is shown in Fig. 2. We see that light-induced

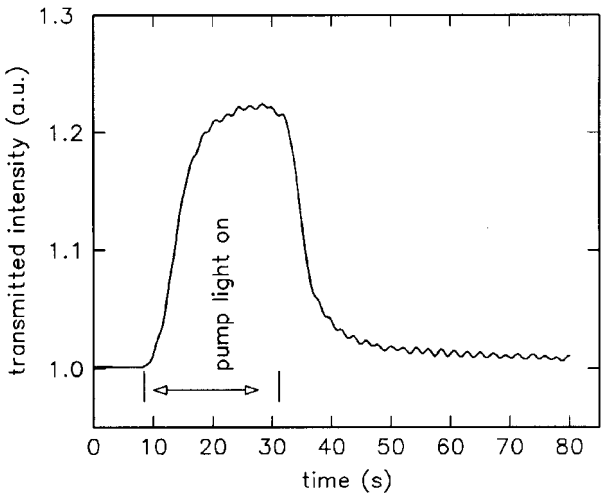

Fig. 2. Intensity of transmitted probe beam (polarized along the *a*-axis) with and without pump beam at room temperature. The pump beam ($\lambda = 51.45$ nm, $I_{\mathrm{R}} = 10$ W/cm^2) is switched on at $t = 8$ s and turned off at $t = 30$ s

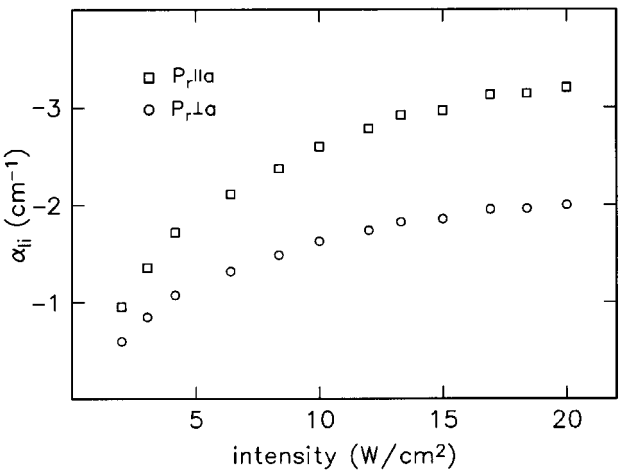

Fig. 3. Light-induced adsorption α_{li} as a function of pump-beam power density. The polarization of the pump beam is along the *a*-axis, and that of the probe beam (P_{r}) is either perpendicular (*circles*) or parallel (*squares*) to the *a*-axis

transparency occurs in our sample. The steady-state values of α_{li} for the He-Ne probe beam as a function of pump intensity are presented in Fig. 3. The polarization of the pump beam has almost no influence on α_{li} (not shown in the figure because there is no notable difference), whereas α_{li} is about 1.6 times larger for the probe beam polarized along the *a*-axis than for the probe beam polarized perpendicular to *a*-axis. Similar dependences on polarization have also been reported for other crystals, e.g., strontium-barium niobate [7, 8].

2.2 Holographic experiments

2.2.1 Dependence on polarization of the writing beams. In contrast to the refractive-index grating, modulation of the absorption grating is insensitive to the polarization of both writing beams. Figure 4 shows the buildup of the absorption grating as well as the complementary refractive-index grating for differing polarization under the following experimental conditions: $\lambda = 514.5\,\mathrm{nm}$, $\Lambda = 0.6\,\mu\mathrm{m}$ and $I_0 = 1.2\,\mathrm{W/cm^2}$. It can be seen from the figure that $\Delta\alpha$ remains almost unchanged, while Δn is doubled when polarization of both beams is relocated from along the *b*-axis to the *a*-axis. The favorable configuration for recording of the refractive-index grating is chosen in the following experiments, i.e., the grating vector is along the *a*-axis and the polarization of both beams is in the plane of incidence. From Fig. 4 we see that the response times of both gratings are of the same order, but much larger than that of the primary grating as already reported [4].

2.2.2 Dependence on wavelength. It is interesting to note that the absorption gratings can be either in phase or shifted by 180° with respect to the light pattern at the same grating spacing and light intensity, depending on the wavelength as given in Table 1. In this experiment, the half-crossing angle θ is 7° and the total-incident intensity I_0 is $1.2\,\mathrm{W/cm^2}$. However, under these conditions, the phase shift of the refractive-index grating with respect to the light pattern remains around 90° and thus the direction of energy transfer in beam coupling does not change. All of the phases measured show a fluctuation of ±20° and the error of the modulation amplitude of the absorption grating is ±15%, which can be attributed to instabilities of the setup.

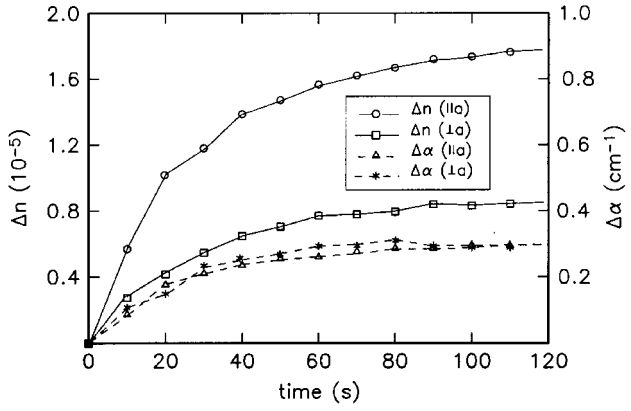

Fig. 4. Build-up of refractive-index and absorption gratings for the polarization of the writing beams parallel and perpendicular to the *a*-axis ($I_0 = 1.2\,\mathrm{W/cm^2}$ and $\Lambda = 0.6\,\mu\mathrm{m}$). The symbols represent the results measured and the curves are guides to the eye

Table 1. Modulation $\Delta\alpha$ and phase Φ_A of the absorption grating at different wavelengths ($I_0 = 1.2\,\mathrm{W/cm^2}$ and $\theta = 7°$)

λ (nm)	514.5	501.7	496.5	488.0	476.5	457.9
$\Delta\alpha$ ($\mathrm{cm^{-1}}$)	0.21	0.19	0.10	0.02	0.07	0.10
Φ_{A} (deg)	180	180	180	0	0	0

2.2.3 Dependence on grating spacing. At identical wavelength, modulation and phase of the absorption grating also depend on grating spacing. For example, under the conditions $\lambda = 514.5\,\mathrm{nm}$ and $I_0 = 1.2\,\mathrm{W/cm^2}$, the measured values $\Delta\alpha$ and Φ_{A} of the absorption grating strongly depend on Λ, as listed in Table 2. We can see that a decrease in grating spacing can change the phase shift of the absorption grating from 180° to 0° with respect to the light pattern.

Under proper experimental conditions, the absorption grating may disappear. For example, at $\lambda = 514.5\,\mathrm{nm}$, $\Lambda = 1.3\,\mu\mathrm{m}$ and $I_0 = 1.2\,\mathrm{W/cm^2}$, there remains only a refractive-index grating.

2.2.4 Dependence on light intensity. To study the dependence of $\Delta\alpha$ on light intensity, two different grating spacings ($\Lambda = 0.6$ and $1.8\,\mu\mathrm{m}$) are chosen and $\Delta\alpha$ is measured as a function of intensity as shown in Fig. 5. For the grating spacing $\Lambda = 0.6\,\mu\mathrm{m}$, the absorption gratings are always in phase

Table 2. Dependence of modulation $\Delta\alpha$ and phase Φ_A of the absorption grating on grating spacing Λ at $\lambda = 514.5\,\mathrm{nm}$ and $I_0 = 1.2\,\mathrm{W/cm^2}$

Λ (μm)	2.1	1.5	1.0	0.8	0.5
$\Delta\alpha$ ($\mathrm{cm^{-1}}$)	0.21	0.10	0.20	0.25	0.36
Φ_{A} (deg)	180	180	0	0	0

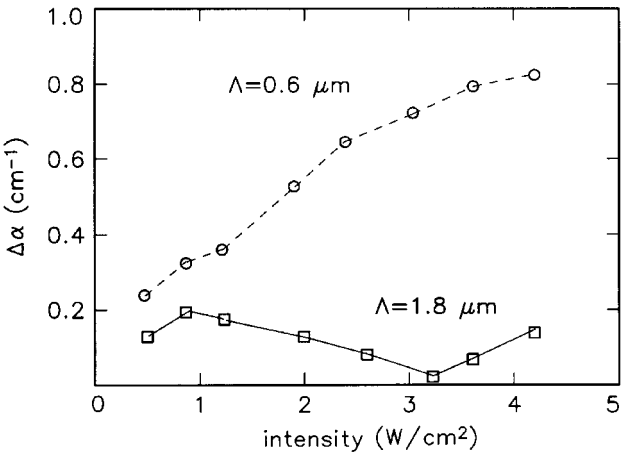

Fig. 5. Dependence of $\Delta\alpha$ on light intensity for absorption gratings with grating spacings $\Lambda = 0.6$ and $1.8\,\mu\mathrm{m}$. The symbols represent the results measured and the curves are guides to the eye. The phase shift of the absorption grating with $\Lambda = 0.6\,\mu\mathrm{m}$ is always 0 with respect to the light pattern. For the grating with $\Lambda = 1.8\,\mu\mathrm{m}$, the phase shift is 180° for $I_0 < 3\,\mathrm{W/cm^2}$ and 0 for $I_0 > 3\,\mathrm{W/cm^2}$

with respect to the light pattern and the increase in intensity leads to a rise in absorption modulation. At low intensity, the absorption grating with a spacing of $\Lambda = 1.8\,\mu\mathrm{m}$ is phase-shifted by 180° with respect to the light pattern, but for $I_0 > 3\,\mathrm{W/cm^2}$, the phase changes from 180° to 0°. As can be seen in Fig. 5, the increase in intensity does not always lead to a larger amplitude of the absorption grating with $\Lambda = 1.8\,\mu\mathrm{m}$, although the light-induced absorption change increases with light intensity.

3 Analyses and discussion

In our previous paper [4], we have reported on properties of refractive-index gratings in $Bi_4Ti_3O_{12}$ and concluded that the redistribution of photoexcited charges forms a space-charge field which modulates the refractive index via the linear electro-optic effect. According to the Kramers-Kronig relation [9], a modulation of the refractive index is associated with a change of absorption and vice versa. If this causes the absorption grating, then the gratings (absorption and refractive index) should have the same dependencies on experimental parameters such as intensity, grating spacing etc.. However, besides the response time constants which can be estimated to be approximately of the same order for the complementary refractive-index and absorption grating as illustrated in Fig.4, all other experimental results show that both gratings do not have the same origin. In particular, a Kramers-Kronig contribution of the absorption resulting from the refractive-index grating should have a phase shift of 90° (and not of 0 or 180°).

Our results concerning the light-induced absorption changes can be explained by additional shallow traps that may be involved in the formation of holographic gratings. As in other photorefractive crystals, if there are shallow traps, the redistribution of beam intensity can cause a shallow-trap grating that is either in phase or shifted by 180° with respect to the light pattern. Since the magnitude of the change in absorption is proportional to the density of filled shallow traps, the shallow-trap grating induces a modulation of absorption. As described by Tayebati and Mahgerefteh [10], in the absence of an applied field, modulation charge density in the shallow trap is given by

$$M_1 = \frac{m M_\mathrm{E}}{\left(1+\frac{\beta}{s_\mathrm{T} I_0}\right)} \frac{1}{\left(k^2+k_0^2\right)} \left(-k^2 + \frac{\beta}{s_\mathrm{T} I_0} k_{0\mathrm{D}}^2\right), \tag{5}$$

where m is the light intensity modulation, β the thermal excitation rate from the shallow traps, s_T the light-excitation cross section for shallow traps, $k = 2\pi/\lambda$ the amplitude of the grating vector, and the other parameters are defined as follows:

$$N_\mathrm{E} = \frac{(N_\mathrm{D} - N_\mathrm{A} - N_0)\,(N_\mathrm{A} + N_0)}{N_\mathrm{D}},$$

$$M_\mathrm{E} = \frac{M_0\,(M_\mathrm{T} - M_0)}{M_\mathrm{T}}, \tag{6}$$

$$k_{0\mathrm{D}}^2 = \frac{e^2 N_\mathrm{E}}{\epsilon k_\mathrm{B} T}, \qquad k_{0\mathrm{T}}^2 = \frac{e^2 M_\mathrm{E}}{\epsilon k_\mathrm{B} T}, \tag{7}$$

$$k_0^2 = k_{0\mathrm{D}}^2 + k_{0\mathrm{T}}^2. \tag{8}$$

Here, N_D is the density of donors, N_A the density of acceptors, M_T the total shallow-trap density, M_0 the mean density of filled shallow traps, N_0 the mean density of ionized donors, ϵ the dielectric constant along the direction of charge migration, e the elementary charge, and $k_\mathrm{B}T$ the thermal energy.

The above equations hold for both p-type and n-type crystals. The first term of (5) corresponds to the transfer of charges by diffusion, and the second term originates from the transfer of charges from deep-level centers to shallow traps. As we know, the transfer of charges by direct photoexcitation leads to a charge density in phase with respect to the light pattern while diffusion always yields a charge density phase-shifted by 180° with respect to the light pattern. As shown in Fig. 6, M_1 can be both positive and negative, which corresponds to a charge-density modulation in phase or shifted by 180° with respect to the light pattern. The modulation $\Delta\alpha$ of the absorption grating can be written as

$$\Delta\alpha = (s_\mathrm{T} - s_\mathrm{D})\, M_1, \tag{9}$$

where s_D is the cross section for the excitation of donors. The dependence of $\Delta\alpha$ on Λ is also shown in Fig. 6. Here, positive $\Delta\alpha$ indicates an absorption grating in phase while negative $\Delta\alpha$ corresponds to an absorption grating shifted by 180° with respect to the light pattern. Figure 6 is merely an example that shows the relations of M_1 and $\Delta\alpha$ as functions of grating spacing at different intensities [(5)–(9)]. In the calculation, the variation of parameters does not change the variation tendency of M_1 and thus of $\Delta\alpha$, i.e., M_1 increases with Λ, because diffusion becomes weaker at larger grating spacings and thus the first term in (5) decreases.

We define the parameter $\Lambda_0(I_0) = (2\pi/k_{0\mathrm{D}})(s_\mathrm{T} I_0/\beta)^{1/2}$. If $\Lambda = \Lambda_0(I_0)$ is satisfied in the experiment, then $M_1 = 0$ and $\Delta\alpha = 0$. For our example with light-induced transparency at room temperature, the phase of the absorption grating with respect to the light pattern obeys the following relations

$$\Phi_\mathrm{A} = 180°\,(\Lambda > \Lambda_0(I_0)) \text{ and } \Phi_\mathrm{A} = 0\,(\Lambda < \Lambda_0(I_0)) \tag{10}$$

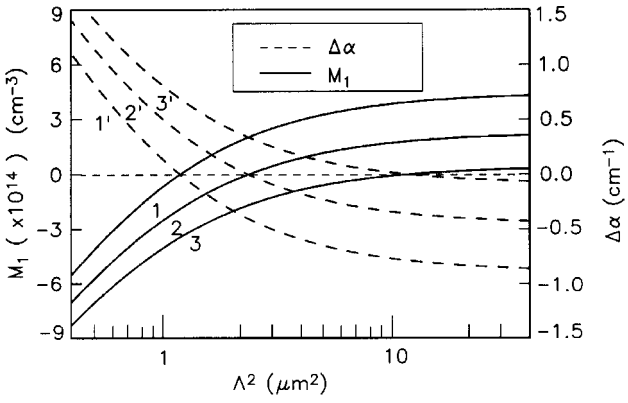

Fig. 6. Examples of the modulation M_1 of a steady-state shallow-trap charge density grating and the modulation $\Delta\alpha$ of the absorption grating as a function of grating spacing Λ for different intensities [(5)–(9)]: $I_0 = 0.5\,\mathrm{W/cm^2}$ (curves 1 and 1'), $I_0 = 1\,\mathrm{W/cm^2}$ (curves 2 and 2') and $I_0 = 5\,\mathrm{W/cm^2}$ (curves 3 and 3'). The other parameters are $\beta = 10\,\mathrm{Hz}$, $N_\mathrm{A} = 1.9\times10^{15}\,\mathrm{cm^{-3}}$, $M_\mathrm{T} = 1.9\times10^{16}\,\mathrm{cm^{-3}}$, $N_\mathrm{D} = 10^{19}\,\mathrm{cm^{-3}}$, $\gamma_\mathrm{D}/\gamma_\mathrm{T} = 0.5$, $\epsilon = 120$, $s_\mathrm{T} = 2\times10^{-15}\,\mathrm{cm^2}$ and $s_\mathrm{D} = 10^{-15}\,\mathrm{cm^2}$

From Table 2 we know that the phase of the absorption grating changes from 180° to 0 with decreasing grating spacing Λ, i.e., $\Lambda_0(I_0 = 1.2\,\mathrm{W/cm^2})$ is between 1.5 and 1.0 μm; the result measured (Sect. 2.2.3) is $\Lambda_0(I_0 = 1.2\,\mathrm{W/cm^2}) = 1.3\,\mu\mathrm{m}$. The intensity dependence of the modulation of absorption grating can also be qualitatively explained with Fig. 6. From the definition of $\Lambda_0(I_0)$, we know that the increase in intensity leads to a rise in $\Lambda_0(I_0)$. For a grating with small grating spacing Λ, $\Lambda_0(I_0)$ may always be larger than the grating spacing and the phase shift of the absorption grating is 0. For a grating with large grating spacing, $\Lambda = 1.8\,\mu\mathrm{m}$ for example, $\Lambda_0(I_0)$ may be either smaller or larger than the grating spacing, depending on the intensity so that the increase of intensity may yield a 180° change in the phase of the absorption gratings.

In conclusion, absorption gratings have been studied in a $Bi_4Ti_3O_{12}$ crystal by the beam coupling technique. Amplitude and phase of the absorption grating with respect to the light pattern have been measured at different wavelengths, grating spacings and light intensities. From the experimental results, we can conclude that the absorption grating originates from a redistribution of charges in shallow traps.

Acknowledgements. Financial support by the Deutsche Forschungsgemeinschaft (SFB 225, A6) and a scholarship of the Friedrich-Ebert-Stiftung are gratefully acknowledged.

References

1. S.A. Keneman, A.G.W. Taylor: Ferroelectrics **1**, 227 (1970)
2. S.A. Keneman, A. Miller, G.W. Taylor: Appl. Opt. **9**, 2279 (1970)
3. X. Yue, F. Mersch, R.A. Rupp, U. Heliwig, M. Simon: Phys. Rev. B **53**, 8967 (1996)
4. X. Yue, J. Xu, F. Mersch, R.A. Rupp, E. Kratzig: Phys. Rev. B **55**, 9495 (1997)
5. K. Sutter, P. Günter: J. Opt. Soc. Am. B **7**, 2274 (1990)
6. F. Kahmann: J. Opt. Soc. Am. A **10**, 1562 (1993)
7. K. Buse, R. Prankrath, E. Krätzig: Opt. Lett. **19**, 260 (1994)
8. S. Orlov, M. Segev, A. Yariv, R.R. Neurgaonkar: Opt. Lett. **12**, 1293 (1994)
9. H.J. Eichler, P. Günter, D.W. Pohl: Laser-Induced Dynamic Gratings. (Springer, Berlin, Heidelberg, 1986)
10. P. Tayebati, D. Mahgerefteh: J. Opt. Soc. Am. B **8**, 1053 (1991)